An unprecedented route of ·OH radical reactivity evidenced by an electrocatalytical process: Ipso-substitution with perhalogenocarbon compounds

Emmanuel Mousset[a,b], Nihal Oturan[a], Mehmet A. Oturan[a,*]

[a] Université Paris-Est, Laboratoire Géomatériaux et Environnement (LGE), EA 4508, UPEM, 5 bd Descartes, 77454 Marne-la-Vallée Cedex 2, France
[b] Laboratoire Réactions et Génie des Procédés, UMR CNRS 7274, Université de Lorraine, 1 rue Grandville BP 20451, 54001 Nancy cedex, France

ARTICLE INFO

ABSTRACT

Hydroxyl radical (·OH) is ubiquitous in the environment and in metabolism. It is one of the most powerful oxidants and can react instantaneously with surrounding chemicals. Currently, three attack modes of ·OH have been identified: hydrogen atom abstraction, addition to unsaturated bond and electron transfer. Perhalogenocarbon compounds such as CCl_4 are therefore supposed to be recalcitrant to ·OH as suggested by numerous authors due to the absence of both hydrogen atom(s) and unsaturated bond(s). Here, we report for the first time a fourth attack mode of ·OH through ipso-substitution of the halogen atom. This breakthrough offers new scientific insight for understanding the mechanisms of ·OH oxidation in the related research areas of research. It is especially a great progress in organic contaminants removal from water. In this study, CCl_4 is successfully degraded and mineralized in aqueous media using a green and efficient electrocatalytical production of homogeneous and heterogeneous ·OH. Maximum degradation rate of 0.298 min^{-1} and mineralization yield of 82% were reached. This opens up new possibilities of emerging water pollutants elimination such as fluorosurfactants.

1. Introduction

The omnipresence of hydroxyl radical (·OH) is now well established in various types of environments including natural waters, atmosphere in which it plays a role of "detergent", interstellar space as well as biological systems where ·OH has an important role in immunity metabolism [1–4]. It makes ·OH as the most important free radical in chemistry and biology because of its multiple implications and applications [5,6].
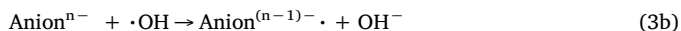
In water media, ·OH is the second strongest oxidizing agent after fluorine with a standard redox potential of 2.8 V/SHE [7]. The presence of unpaired electron on oxygen atom makes ·OH a very reactive species with a mean lifetime estimated as only a few nanoseconds in water [8]. It destroys most of organic and organometallic pollutants until total mineralization, i.e. conversion into CO_2, H_2O, and inorganic ions; hence the interest of its use in water treatment area. Indeed, the occurrence of hazardous and toxic pollutants into the water compartments led the water and wastewater regulatory requirements to become more stringent regarding the release of such compounds. Being xenobiotic, these contaminants cannot be removed by conventional wastewater treatment plant and therefore an advanced physicochemical treatment is

required. Thus, since more than 30 years the outstanding properties of ·OH have been tested for water purification in the so-called advanced oxidation processes (AOPs) [9]. AOPs have gained increasing interests as they constitute promising, efficient and environmental-friendly methods to remove persistent organic pollutants (POPs) from waters [10,11]. Several types of AOPs have been developed based on the *in situ* formation of ·OH by means of various chemical, photochemical, sonochemical, or electrochemical reactions. Then, the ·OH formed can react according to three possible reaction modes proposed in literature: (i) hydrogen atom abstraction (dehydrogenation), (ii) electrophilic addition to an unsaturated bond (hydroxylation) and (iii) electron transfer (redox) reactions [6,10]. The first mode is typical for alkanes and alcohols (Eq. (1)) with rate constants in the range 10^6–$10^8 M^{-1} s^{-1}$ [12], whereas the second mode occurs especially with aromatics (ArH) (Eq. (2a)-(2b)) with rate constants as high as 10^8–$10^{10} M^{-1} s^{-1}$ [12] while the third mode is generally given with oxidizable inorganics such as cation (Fe^{2+} (Eq. (3a))) as well as anions (Eq. (3b)) (Cl^-, NO_2^-, HCO_3^-) and organics (Eq. (4)) [1]:
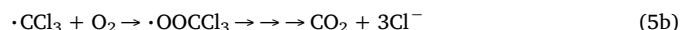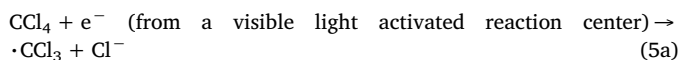
$$RH + ·OH \rightarrow R· + H_2O \tag{1}$$

$$ArH + \cdot OH \rightarrow ArHOH \cdot \tag{2a}$$

$$ArHOH \cdot + O_2 \rightarrow ArOH + HO_2 \cdot \tag{2b}$$

$$Fe^{2+} + \cdot OH \rightarrow Fe^{3+} + OH^- \tag{3a}$$

$$Anion^{n-} + \cdot OH \rightarrow Anion^{(n-1)-} \cdot + OH^- \tag{3b}$$
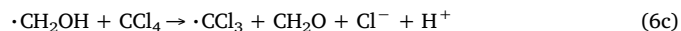
$$RH + \cdot OH \rightarrow RH \cdot^+ + OH^- \tag{4}$$

Therefore, $\cdot OH$s are very active species that can oxidize even the most recalcitrant chemicals. However, $\cdot OH$ have been considered in several studies as unreactive with perhalogenated alkanes (C_xX_y) water contaminants that contain only carbon and halogen atoms such as carbon tetrafluoride (CF_4), carbon tetrachloride (CCl_4), hexa-fluoroethane (C_2F_6) and hexachloroethane (C_2Cl_6) that are widely used as etchant in semiconductor manufacturing and as refrigerants. Indeed, these pollutants do not have any hydrogen atom as well as no un-saturated bond. Thus, no one of the three above-mentioned modes of $\cdot OH$ actions can occur.

Interestingly, several authors intended to be able to degrade per-halogenocarbon compounds by applying some AOPs but in the presence of an organic precursor. Cho et al. [13,14] succeeded to degrade CCl_4 with a heterogeneous photocatalysis (UV/TiO$_2$) process in the presence of surfactant as organic precursor. It was proposed as a hypothesis that a complex formation between the surfactant functional groups and TiO$_2$ surface was responsible for the weak visible light absorption and the subsequent photo-induced electron transfer to CCl_4 (Eq. (5a)-(5b)):

$$CCl_4 + e^- \text{ (from a visible light activated reaction center)} \rightarrow \cdot CCl_3 + Cl^- \tag{5a}$$

$$\cdot CCl_3 + O_2 \rightarrow \cdot OOCCl_3 \rightarrow \rightarrow \rightarrow CO_2 + 3Cl^- \tag{5b}$$

Gonzalez et al. [15] employed methanol as precursor to mineralize CCl_4 by H_2O_2 photolysis according to the following reactions sequence (Eq. (6a)-(6c)):

$$H_2O_2 + h\nu \text{ (254 nm)} \rightarrow 2 \cdot OH \tag{6a}$$

$$\cdot OH + CH_3OH \rightarrow \cdot CH_2OH + H_2O \tag{6b}$$

$$\cdot CH_2OH + CCl_4 \rightarrow \cdot CCl_3 + CH_2O + Cl^- + H^+ \tag{6c}$$

In addition, some authors applying other AOPs also demonstrated the degradation of CCl_4 by suggesting the formation of additional in-organic species that were responsible for its decomposition. Thus, it was considered that sonication decomposes water molecules into hydrogen radical ($\cdot H$) and $\cdot OH$ and then CCl_4 reacts with $\cdot H$ [16,17]:

$$H_2O +))) \rightarrow \cdot H + \cdot OH \tag{7a}$$

$$CCl_4 + \cdot H \rightarrow HCl + \cdot CCl_3 \tag{7b}$$
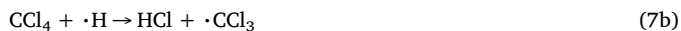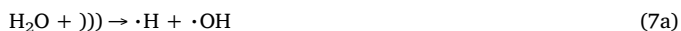
In a modified chemical Fenton's treatment it was suggested that the superoxide ion ($O_2 \cdot^-$) was responsible for the decomposition of CCl_4 [18–20]. $O_2 \cdot^-$ is a weak nucleophile and reductant that was suggested to be able to degrade CCl_4 in aprotic media such as dimethyl sulfoxide and dimethylformamide as organic precursor [21,22] and more re-cently in aqueous media by using high concentration of H_2O_2 (> 0.1 M) in a Fenton-like process.

However, an important feature is that at the operated Fenton pH (pH 3 initially), hydroperoxyl ion ($HO_2 \cdot$), a weak oxidant ($E^\circ = 1.65$ V/ SHE), predominate in such acidic conditions ($pKa = 4.8$) instead of $O_2 \cdot^-$ [23]. Therefore, the role of $O_2 \cdot^-$ has to be reconsidered.

Recently, electrochemical advanced oxidation processes (EAOPs) for generating $\cdot OH$ in a catalytic and continuous mode have gained increasing interests [23–27]. They are not only more environmentally friendly as electron is a clean reagent but also more efficient as they can even degrade the most recalcitrant compounds [28–34] such as cya-nuric acid known to be resistant to $\cdot OH$ oxidation in more conventional AOPs [35]. Another advantage is that EAOPs are modular process

according to the electrodes materials to be used which lead to different oxidizing/reducing species formed [23,36–40]. In other words, the nature of the electrogenerated species can be controlled by the ade-quate electrode materials and operating conditions. Therefore, the oxidative degradation of perhalogenated compounds such as CCl_4 has never been studied by EAOPs, it appears important to carry out it as it can bring novel tremendous scientific insights on the mechanism of degradation of such molecules according to the electrode material employed.

2. Experimental

2.1. Chemicals

All the chemicals were of analytical grade, and were used without any further purification. Carbon tetrachloride (CCl_4), titanium tetra-chloride ($TiCl_4$), potassium hydrogen phthalate, hydrogen peroxide (H_2O_2) (30% w/w) and sodium sulfate (Na_2SO_4) were purchased from Sigma-Aldrich. Heptahydrated ferrous sulfate ($FeSO_4 \cdot 7H_2O$), sulfuric acid (H_2SO_4) and phosphoric acid (H_3PO_4) (85% w/w) were supplied by Acros Organics. In all experiments, the solutions were prepared with ultrapure water from a Millipore Simplicity 185 (resistivity > 18 MΩ cm at room temperature).

2.2. Electrochemical reactor set-up

Electrolysis experiments with CCl_4 aqueous solutions (0.2 mM) were run at controlled temperature (22.0 ± 0.1 °C), in a 0.20 L closed-un-divided glass electrochemical reactor under current-controlled condi-tions. The cathode was either a 150 cm^2 carbon felt (CF) piece (Carbone-Lorraine, France) or a 28 cm^2 plate of stainless steel (SS) (GoodFellow, France). Either a Pt grid (5 cm height cylindrical (i.d. = 3 cm)) or boron-doped diamond (BDD) coated on a Niobium (Nb) plate (28 cm^2) (Condias, Germany) was employed as an anode material with an electrode distance of 3.5 cm. The electrochemical cell was monitored by a power supply HAMEG 7042-5 (Germany) and the applied current was set to 1000 mA. An inert supporting electrolyte (Na_2SO_4 at 0.050 M) was added to the medium to ensure a constant ionic strength (0.15 M). The pH of the initial solution was adjusted to a pH of 3 [41]. The solutions were continuously stirred to assure homo-geneous mixing. $FeSO_4 \cdot 7H_2O$ was added (0.05 mM) as a source of cat-alyst (Fe^{2+}) to implement Fenton's reaction in EF process. Compressed air was bubbled initially before starting the experiment and before adding CCl_4 compound [42]. This was to saturate the aqueous solution in O_2 as a source of H_2O_2 production (Eq. (9)) while avoiding the vo-latilization of CCl_4. The reactor set-up for electrolysis experiments is illustrated in Fig. 1. The same reactor was employed to perform H_2O_2 oxidation experiments, except that the electrodes were absent.

2.3. Analytical methods

2.3.1. Cyclic voltammetry (CV)

CV experiments were performed to evaluate the electroactivity of CCl_4 in aqueous media with a potentiostat/galvanostat PGP201 VoltaLab (Radiometer Analytical S.A.) in a three-electrode system. Either Pt (1 mm diameter) or glassy carbon (3 mm diameter) was em-ployed as working electrode while a Pt wire was used as counter electrode. A saturated calomel electrode (SCE) was employed as re-ference electrode; therefore, all the voltage values given in the text are expressed in V/SCE, unless stated otherwise. Sodium sulfate (0.050 M) was used as electrolyte and the solutions were acidified to pH 3.0, the optimal EAOPs conditions. The CV experiments were performed in a voltage range of −3.0 V to +3.0 V and at a scan rate of 10 mV s^{-1}.

2.3.2. Hydrogen peroxide experiments and analysis

The oxidation power of H_2O_2 onto CCl_4 was evaluated by adding
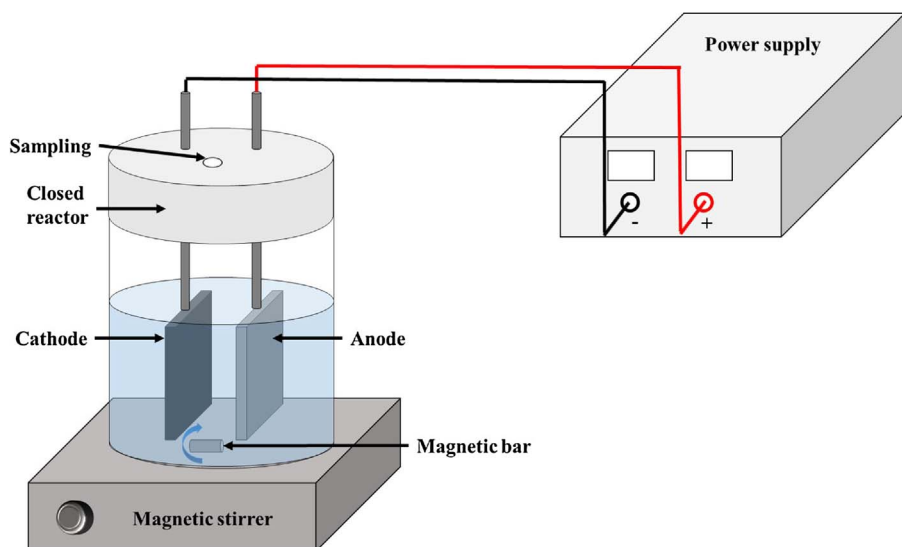
Fig. 1. Reactor set-up for H_2O_2 oxidation and electrolysis experiments.

initially H_2O_2 in excess (100 mM) into CCl_4 (0.2 mM) aqueous solution before starting the experiments. The amount of H_2O_2 accumulated in bulk solution was determined by performing electrolysis experiments in the same conditions than EAOPs treatments, except that no Fe^{2+} was added to avoid Fenton's reaction to occur [37]. H_2O_2 was quantified by colorimetry using $TiCl_4$ [43]. The absorbance of the pertitanic acid complex formed was measured with a Perkin Elmer (USA) Lambda 10 UV–vis spectrophotometer at a wavelength of 410 nm. An external calibration curve was obtained with standards of H_2O_2, giving a molar extinction coefficient of around $935 \pm 2 \, L \, mol^{-1} \, cm^{-1}$. The H_2O_2 concentrations were then calculated according to the Beer-Lambert law.

2.3.3. Total organic carbon (TOC) measurements

TOC analyses were performed to quantify the mineralization degree during the different kind of treatments. The solution TOC values were determined by thermal catalytic oxidation (680 °C in presence of Pt catalyst) using a Shimadzu (Japan) V_{CSH} TOC analyzer. All samples were acidified to pH 2 with H_3PO_4 (25% w/w) to remove inorganic carbon. The injection volumes were 50 μL. Calibrations were performed by using potassium hydrogen phthalate solutions ($50 \, mg \, C \, L^{-1}$) as standard. All measured TOC values were given with a coefficient of variance below to 2%.

Mineralization yields (r_{min}) were considered equivalent to TOC removal percentage and can be determined according to the following Eq. (8):

$$r_{min}(\%) = \frac{(\Delta TOC)_t}{TOC_0} \times 100$$

(8)

where $(\Delta TOC)_t$ is the difference between the initial TOC (TOC_0) and TOC at time t.

2.3.4. Ionic chromatography analysis

The inorganic ions released in the treated solutions were determined by ion chromatography using a Dionex ICS-1000 basic ion chromatography system (USA). The analysis of anions was monitored using an IonPac AS4A-SC (25 cm × 4 mm) anion-exchange column linked to an IonPac AG4A-SC (5 cm × 4 mm) column guard. The system was equipped with a DS6 conductivity detector containing a cell heated at 35 °C. The mobile phase contained 1.8 mM Na_2CO_3 and 1.7 mM NaHCO₃. The flow rate was set to $2 \, mL \, min^{-1}$. The suppressor SRS (Self Regenerating Suppressor) needed to prevent the influence of the eluent ions in the detector signal was at a current of 30 mA.

2.3.5. Kinetic model for CCl_4 degradation

The decay rate of CCl_4 can be written as follow (Eq. (9)):

$$\frac{d[CCl_4]}{dt} = -k_{CCl4}[^{\bullet}OH][CCl_4]$$

(9)

where $[CCl_4]$ is the concentration of CCl_4, k_{CCl4} is the decay rate constant of CCl_4 and $[\cdot OH]$ is the concentration of $\cdot OH$ radical.

Considering that the degradation of one mole of CCl_4 produce four moles of Cl^-, the following equivalence of chemical rate can be obtained (Eq. (10)):

$$-\frac{d[CCl_4]}{dt} = +\frac{1}{4}\frac{d[Cl^-]}{dt}$$

(10)

By inserting Eq. (10) into Eq. (9), Eq. (11) is given:

$$\frac{d[Cl^-]}{dt} = 4k_{CCl4}[^{\bullet}OH][CCl_4]$$

(11)

By considering that $[Cl^-] = [CCl_4]_0 - [CCl_4]$, that $[CCl_4] = [CCl_4]_0 - [Cl^-]_{meas}$ and that $[Cl^-] = 4[Cl^-]_{meas}$, the following Eq. (12) is retrieved from Eq. (11):

$$\frac{d[Cl^-]_{meas}}{dt} = k_{CCl4}[^{\bullet}OH]([CCl_4]_0 - [Cl^-]_{meas})$$

(12)

where $[CCl_4]_0$ is the initial concentration of CCl_4 and $[Cl^-]_{meas}$ is the measured concentration of Cl^- released into the solution.

By considering the quasi-steady state approximation towards the $\cdot OH$ concentration evolution, a pseudo-first order kinetic model can be assumed [23]:

$$\frac{d[Cl^-]_{meas}}{dt} = k_{app}([CCl_4]_0 - [Cl^-]_{meas})$$

(13)

where $k_{app} = k_{CCl4}[\cdot OH]$ is the apparent decay rate constant of CCl_4 oxidation by OH.

After integration of Eq. (13), the semi-logarithmic Eq. (14) is obtained:

$$ln\left(\frac{[CCl_4]_0}{[CCl_4]_0 - [Cl^-]_{meas}}\right) = ln\left(\frac{[CCl_4]_0}{[CCl_4]_t}\right) = k_{app}t$$

(14)

where $[CCl_4]_t$ is the concentration of CCl_4 at time t.

3. Results and discussion

3.1. Evaluation of electroactivity of CCl_4

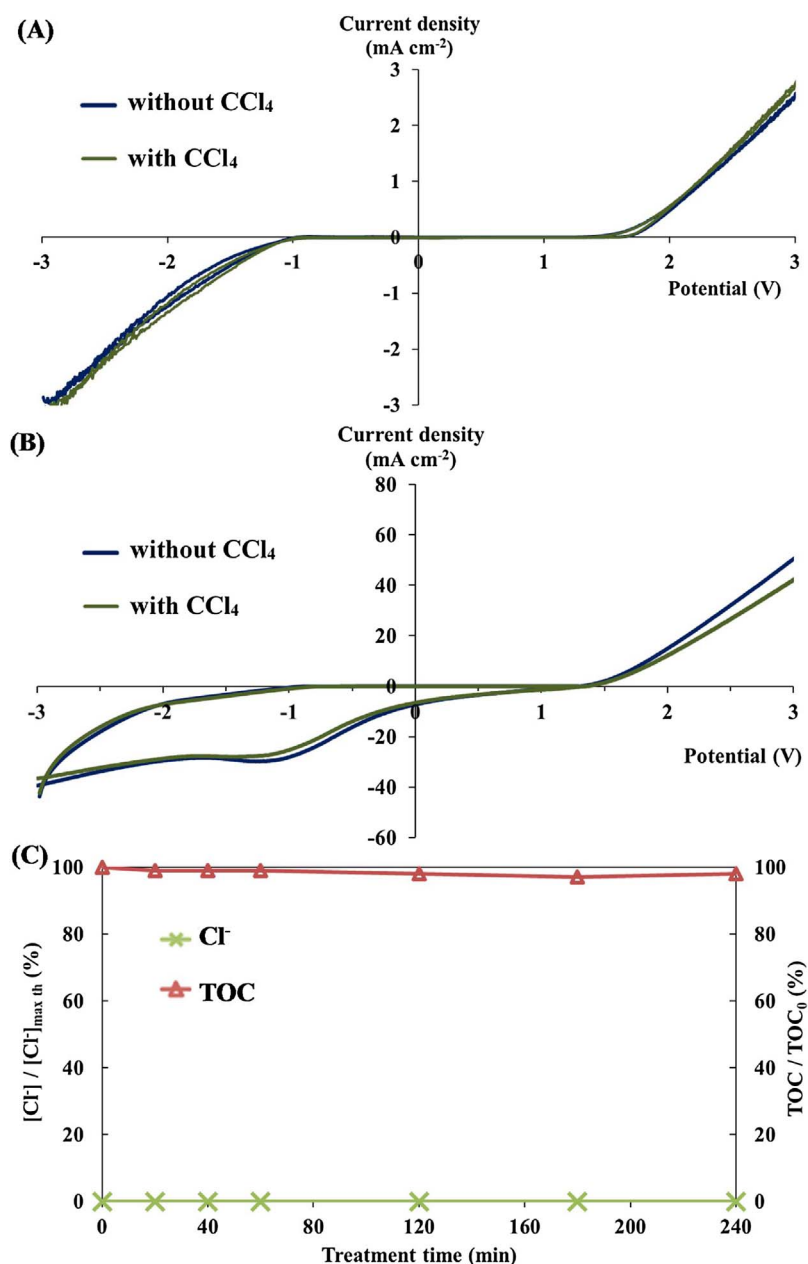Before studying the possibility of CCl_4 degradation by $\cdot OH$

(A)

(B)

(C)

Fig. 2. Evaluation of CCl$_4$ electroactivity and reactivity with H$_2$O$_2$. (A), cyclic voltamogrammes in absence or presence of CCl$_4$ with Pt working electrode (Pt counter electrode); (B), cyclic voltamogrammes in absence or presence of CCl$_4$ with glassy carbon working electrode (Pt counter electrode), (C), oxidative treatment of CCl$_4$ with hydrogen peroxide.

produced by EAOPs, it appeared important to preliminary verify the electroactivity of CCl$_4$ to check if it can be degraded by direct electron transfer at anode or cathode surface. Cyclic voltammetry (CV) have been therefore performed in voltage window ranging from −3 V to +3 V in Na$_2$SO$_4$ (0.050 M) solution at pH 3. Either platinum (Pt) or glassy carbon was used as working electrode, since both electrode materials were later employed in the EAOPs. As anticipated, neither electro-oxidation nor electro-reduction of CCl$_4$ occurred by using Pt as working electrode (Fig. 2A). Whatever the presence or not of CCl$_4$, no peak of current was observed except the oxidation of H$_2$O into O$_2$ (anode) and its reduction into H$_2$ (cathode). Employing vitreous carbon as working electrode further demonstrated the non-electroactivity of CCl$_4$ at the potential range studied (Fig. 2B). A difference was noticed between Pt and carbon electrode, since a cathodic peak, attributed to the formation of H$_2$O$_2$ (Eq. (15)), was noticed at −0.6 V with the latter. This peak is expected because carbonaceous cathodes are well-known to promote the formation of H$_2$O$_2$ from 2-electron reduction of O$_2$ [44]:

$$O_2 + 2H^+ + 2e^- \rightarrow H_2O_2 \tag{15}$$

To further investigate the oxidative inaction of H$_2$O$_2$ towards CCl$_4$, experiments were performed by initially spiking H$_2$O$_2$ in excess (100 mM) in a 0.2 mM CCl$_4$ aqueous solution in a hermetic seal batch reactor (Fig. 2C and Fig. 1). As expected H$_2$O$_2$ was not able to degrade CCl$_4$ as no Cl$^-$ were released in solution while the total organic carbon (TOC) values remained unchanged along the experiment. The H$_2$O$_2$ concentration measurements depicted in Fig. 3 highlights the absence of H$_2$O$_2$ consumption during oxidation experiments with CCl$_4$, as it remained constant (around 100 ± 0.1 mM) all along the experiment. H$_2$O$_2$ is known to be a relatively weak oxidant ($E°$(H$_2$O$_2$/H$_2$O) = 1.8 V/ SHE) [45] that has relatively poor redox abilities which explain its unreliability to oxidize CCl$_4$.

3.2. Degradation of CCl$_4$ by EAOPs

3.2.1. Role of BDD anode: production of heterogeneous ·OH

The performance of EAOPs to degrade CCl$_4$ (0.2 mM) has been tested. Guided by the hypothesis described in Section 3.1 regarding the role of ·OH in the CCl$_4$ degradation, an anodic oxidation (AO)
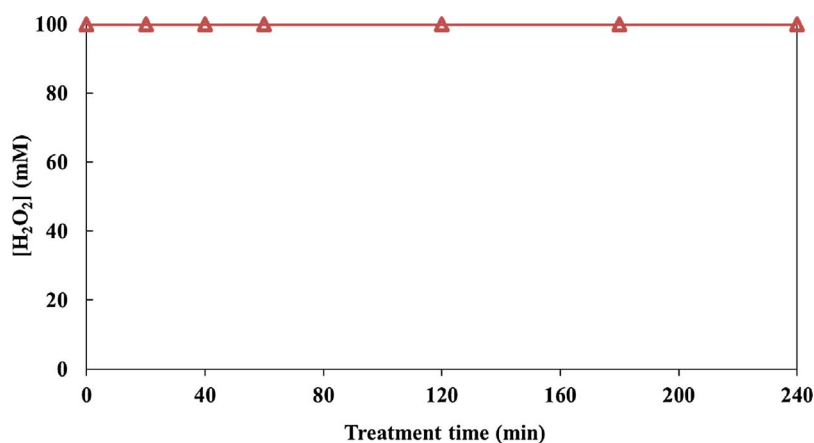
Fig. 3. Hydrogen peroxide concentration evolution during spiking experiment.

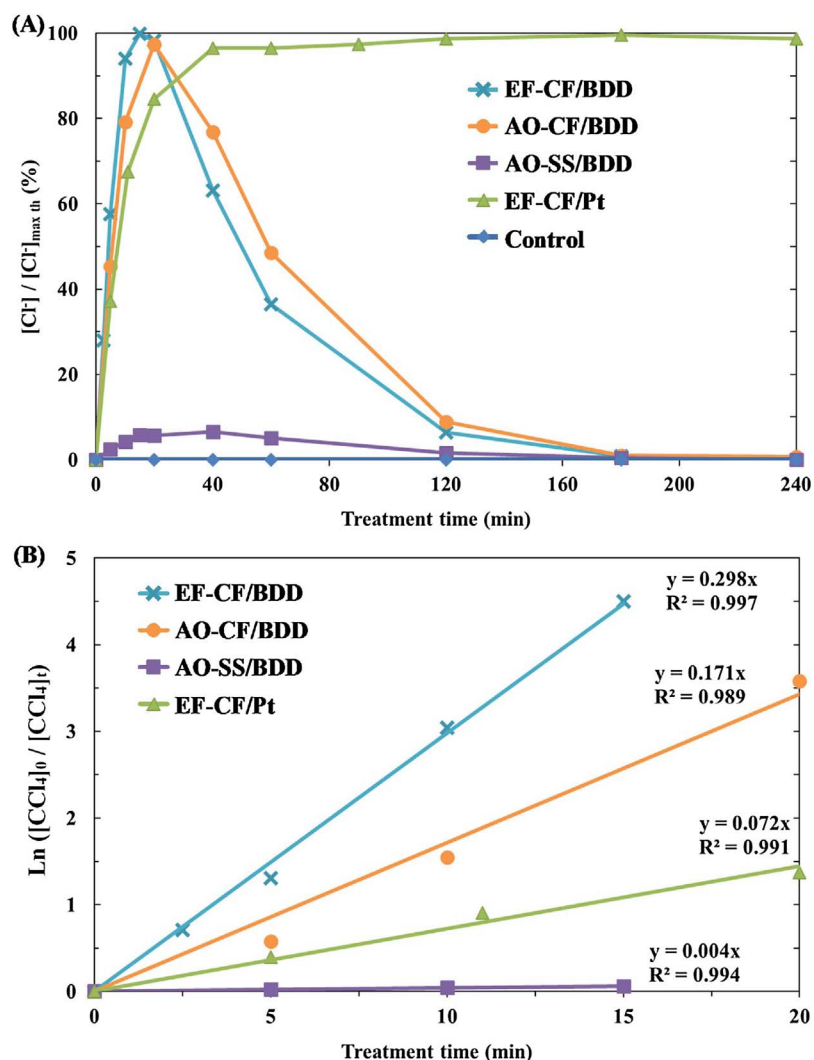**Fig. 4.** Degradation of CCl_4 by AO and EF treatments using different cathodes and anodes. (A), chloride concentration ($[Cl^-]$) evolution normalized by the maximal theoretical Cl^- concentration ($[Cl^-]_{max,th}$) and (B), determination of the apparent rate constants for CCl_4 decay assuming a pseudo-first order kinetic model (SI, Eq. (15)). EF, electro-Fenton; AO, anodic oxidation; CF, carbon felt; SS, stainless steel; BDD, boron-doped diamond.

experiment was first performed with a SS cathode and a BDD anode (AO-SS/BDD cell) in order to check this assumption (Fig. 4A). The experiments were performed in aqueous media, in absence of any other organic compound that could play a role of precursor for $\cdot CCl_3$ formation. Moreover, the electrolysis was carried out in dark conditions to avoid any photo-activity. To check whether H_2O_2 formation occurred at SS cathode, the accumulation of H_2O_2 in bulk solution during electrolysis using SS cathode and Pt anode has been performed and the results are represented in Fig. 5. It is shown that the H_2O_2 concentration could

not reach higher value than 0.041 mM, which is very low. This is attributed to the SS material that do not favor the two electrons-oxygen reduction reaction (ORR) pathway to form H_2O_2 and will rather promote the four electron-ORR pathway that produce H_2O (Eq. (16)) as previously stated [23,43]:

$$O_2 + 4H^+ + 4e^- \rightarrow 2H_2O \qquad (16)$$

Therefore, the use of SS cathode limited the formation of H_2O_2 through O_2 reduction (Eq. (15)) (Fig. 5) while the BDD anode ensured
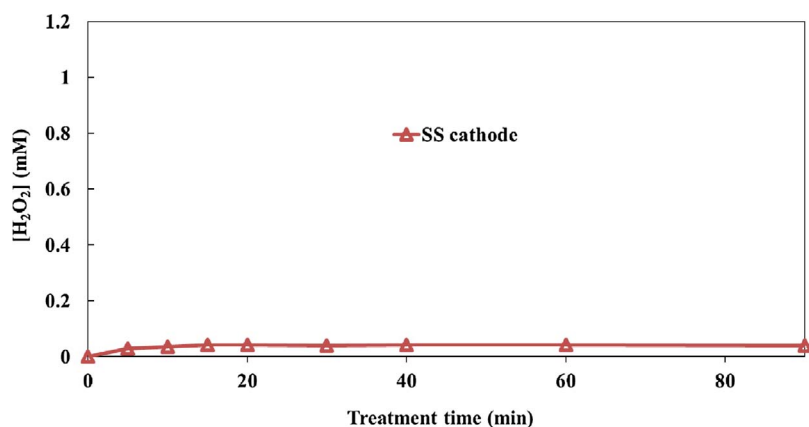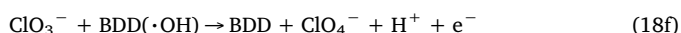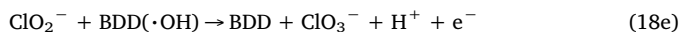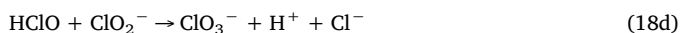
the heterogeneous generation of BDD($\cdot$OH) thanks to its high O_2 evolution overvoltage (2.3 V/SHE) [46,47].

Excitingly, Fig. 4A highlights the release of Cl^- ions into the solution by performing an AO-SS/BDD experiment. Upon control experiments results showing, as expected, the absence of Cl^- ions in solution when no current intensity was applied, CCl_4 was successfully degraded by BDD($\cdot$OH) generated in AO process. It can further be noticed that the amount of Cl^- formed could not reach the maximal Cl^- theoretical concentration ($[Cl^-]_{max,th}$) that could be released. In fact, the rate of chloride formation was in competition with the rate of its oxidation into Cl_2 as highlighted by the decrease of $[Cl^-]$ after 40 min of treatment (Fig. 4A). Indeed, Cl_2 reacts quickly with H_2O to form HOCl [48] that undergoes further oxidation reactions to be converted into chlorate (ClO_3^-) and perchlorate (ClO_4^-) at BDD surface as shown by ionic chromatograms in Fig. 6. Thus, the chromatograms of anions evolution during EF treatment with BDD anode at different treatment time (0 min, 20 min, 40 min, 60 min, 120 min, and 240 min) display Cl^- peaks at retention time around 1.3 min and major peaks of SO_4^{2-} at retention time of 3.1 min. Interestingly, two more peaks could be distinguished at retention times of 2.2 min and 7.4 min, respectively. These peaks are ascribed to chlorine oxyanions such as ClO_3^- and ClO_4^-, respectively. These anions can be formed by Cl^- oxidation into Cl_2 gas at BDD anode due to its high oxidation ability with physisorbed $\cdot$OH formed at its surface (BDD($\cdot$OH)) (Eqs. (17)-(18a)). Cl_2 reacts quickly with H_2O to form the hypochlorous acid (HClO) (Eq. (8b)) in the bulk. Since the pH remained between 2.4 and 3.0 during the whole electrolysis, HClO is the predominant species as compared to $ClO-$ knowing the acid dissociation constant value of HClO; $pKa = 7.54$ (at 25 °C). HClO is then oxidized into ClO_2^- (Eq. (18c)) which is quickly oxidized into ClO_3^- (Eq. (18d)-(18e)) and then into ClO_4^- (Eq. (18f)) as end-product having the maximal oxidation state [49,50]:

$$BDD + H_2O \rightarrow BDD(\cdot OH) + H^+ + e^- \tag{17}$$

$$2Cl^- \rightarrow Cl_2(g) + 2e^- \tag{18a}$$

$$Cl_2(g) + H_2O \rightarrow HClO + H^+ + Cl^- \tag{18b}$$

$$HClO + BDD(\cdot OH) \rightarrow BDD + ClO_2^- + 2H^+ + e^- \tag{18c}$$

$$HClO + ClO_2^- \rightarrow ClO_3^- + H^+ + Cl^- \tag{18d}$$

$$ClO_2^- + BDD(\cdot OH) \rightarrow BDD + ClO_3^- + H^+ + e^- \tag{18e}$$

$$ClO_3^- + BDD(\cdot OH) \rightarrow BDD + ClO_4^- + H^+ + e^- \tag{18f}$$
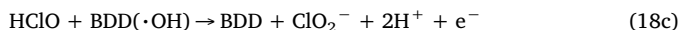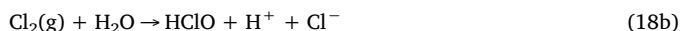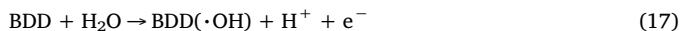
Chlorite ion was not observed in the electrolysis with BDD because the high applied current density (35.7 mA cm^{-2} as reported to the BDD anode surface area) favor the rapid oxidation of ClO_2^- into ClO_3^- as noticed previously [51], especially in BDD experiments performed at 30 mA cm^{-2} [52].

As it can be seen at the detailed view of Cl^- peak evolution

(Fig. 6B), a maximal peak area could be noticed at 20 min of electrolysis, while it started decreasing after longer treatment. At this time the peaks area of ClO_3^- increase until 60 min of treatment and start decreasing after electrolysis time longer than 120 min. In the meanwhile, peaks area of ClO_4^- start raising from 120 min until 240 min of treatment. The subsequent increase/decrease trends observed from Cl^- evolution concentration to ClO_3^- and then to ClO_4^- corroborated the reactions sequence (Eq. (18a)-(18e)).

In addition, the chromatogram of SO_4^{2-} (Fig. 6C) highlights a slight decrease of SO_4^{2-} peak right after the starting of the EF-CF/BDD treatment, corresponding to a SO_4^{2-} concentration decrease from 50 mM to 47.1 ± 0.9 mM. This is attributed to the reaction of SO_4^{2-} with high reactive BDD surface producing sulfate radical ($SO_4\cdot$) (Eq. (19a)) and persulfate ($S_2O_8^{2-}$) (Eq. (19b)) as previously stated [53,54].

$$SO_4^{2-} \rightarrow SO_4\cdot^- + e^- \tag{19a}$$

$$SO_4\cdot^- + SO_4\cdot^- \rightarrow S_2O_8^{2-} \tag{19b}$$
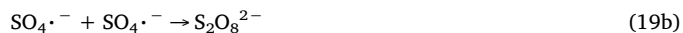
The oxidation power of $SO_4\cdot$ and $S_2O_8^{2-}$ are lower than that of the $\cdot$OH, with standard reduction potentials of 2.6 and 2.01 V/SHE, respectively [23]. It has been previously demonstrated that $SO_4\cdot$ radical could not react with CCl_4, since it was found as one of the end-product during oxidation of chlorinated phenol by $SO_4\cdot$ radical [55]. It means that $\cdot$OH is the only species responsible for the oxidation of CCl_4.

It is important to note that the same trends were observed with all BDD experiments (AO-SS/BDD, AO-CF/BDD and EF-CF/BDD) as these phenomenon depends on the use of BDD anode material itself.

3.2.2. Influence of CF cathode: production of homogeneous $\cdot$OH by peroxone reaction

Interestingly, when a CF cathode was employed (AO-CF/BDD cell), the concentration of Cl^- released could reach $[Cl^-]_{max,th}$ (0.8 mM), highlighting a better degradation of CCl_4 (Fig. 4A). To better understand this behavior, the accumulation of H_2O_2 in bulk solution during electrolysis using CF cathode and Pt anode is represented in Fig. 7. It was first noticed a transient phase followed by a steady state. This phenomenon is typical in undivided cell study and is referred to the competition reactions between H_2O_2 electrogeneration and H_2O_2 decomposition at the anode (Eq. (20a)-(20b)), at the cathode (Eq. (21)) and in a lesser extent decomposition in bulk solution (Eq. (22)) as stated previously by numerous authors [23]:

$$H_2O_2 \rightarrow HO_2\cdot + H^+ + e^- \tag{20a}$$

$$HO_2\cdot \rightarrow O_2 + H^+ + e^- \tag{20b}$$

$$H_2O_2 + 2H^+ + 2e^- \rightarrow 2H_2O \tag{21}$$

$$2H_2O_2 \rightarrow O_2 + 2H_2O \tag{22}$$

It was further emphasized that in presence of CF cathode the
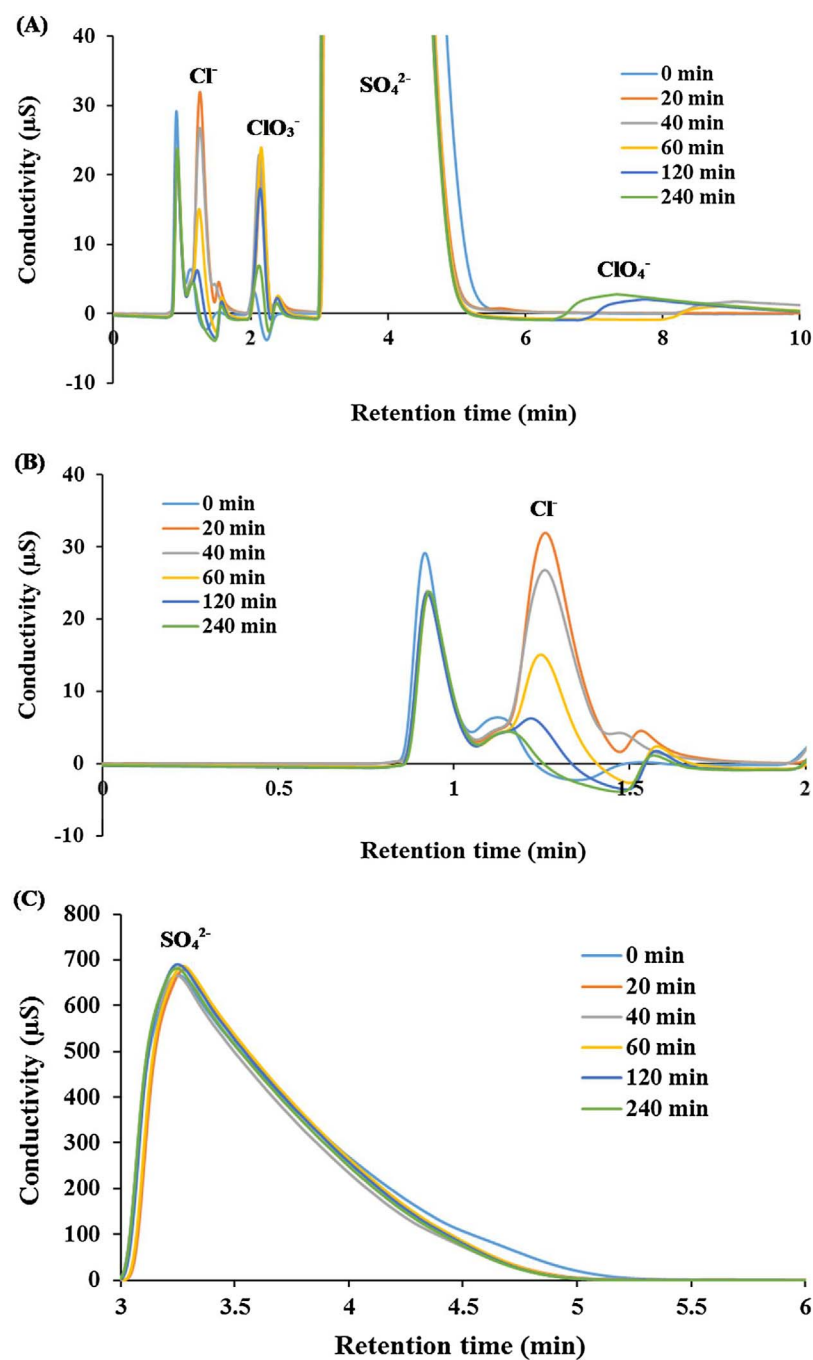
(A)

(B)

(C)

Fig. 6. Chromatograms of anions evolution during EF treatments of CCl_4 with BDD anode (EF-CF-BDD) at different treatment time (0 min, 20 min, 40 min, 60 min, 120 min, 240 min). (A), ionic chromatograms. (B), Cl^- peaks evolution. (C), SO_4^{2-} peaks evolution. Conditions: $I = 1000$ mA, $[Na_2SO_4] = 50$ mM, $[Fe^{2+}] = 0.05$ mM, $V = 200$ mL, pH 3.
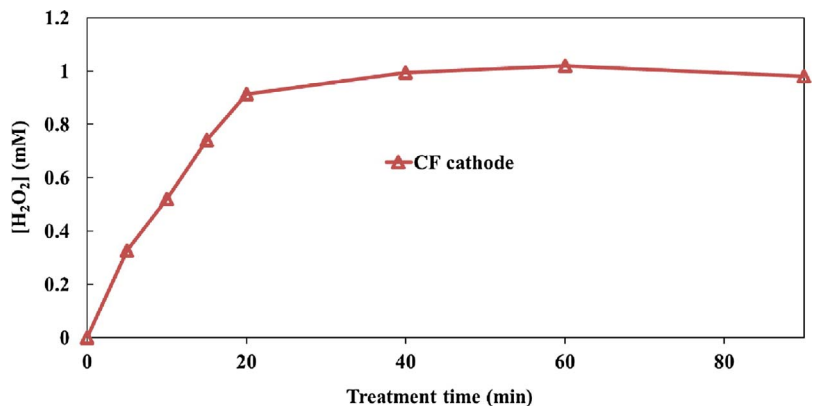

Fig. 7. Hydrogen peroxide accumulation using CF cathode and Pt anode. Conditions: $I = 1000$ mA, $[Na_2SO_4] = 50$ mM, $V = 200$ mL, pH 3.

maximal amount of H_2O_2 accumulated in bulk solution was 1 mM, which was 24 times higher than with SS cathode. It was attributed to the nature of cathode material itself and to its surface area. Indeed, carbon-based cathodes have high H_2 evolution overpotential and low catalytic activity for H_2O_2 decomposition. Moreover, CF has a 3D porous structure that dramatically increases its specific surface area as compared to the SS material employed. This property makes increase the number of active sites for O_2 adsorption before its subsequent reduction into H_2O_2.

Therefore, the enhancement obtained with AO-CF/BDD cell as compared to AO-SS/BDD cell could be due to the additional source of ·OH formed by peroxone reaction between H_2O_2 electrogenerated at CF cathode and O_3 produced at the anode surface (Eq. (23)) [56], as previously shown in several studies performed in similar electrolysis conditions [57–59], thus confirming the role of ·OH in the degradation process.

$$H_2O_2 + 2O_3 \rightarrow 2 \cdot OH + 3O_2 \qquad (23)$$
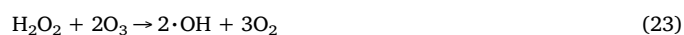
Indeed the high oxidation power of BDD anode allows also generating O_3 from water oxidation at its surface (Eq. (24)) [49].

$$3H_2O \rightarrow O_3 + 6H^+ + 6e^- \qquad (24)$$

It is worthy to specify that O_3 itself is a moderately strong oxidant ($E°(O_3/O_2)$ = 2.1 V/SHE) [45] compared to ·OH and has no direct oxidation effect on CCl_4 as stated by a previous study [19].

3.2.3. Role of iron catalyst: production of homogeneous ·OH by Fenton reaction

The addition of Fe^{2+} (0.1 mM) in order to produce ·OH through Fenton's reaction (Eq. (25)) [23] was further investigated by performing electro-Fenton (EF) treatment with CF cathode and BDD anode (EF-CF/BDD cell).

$$Fe^{2+} + H_2O_2 \rightarrow Fe^{3+} + \cdot OH + OH^- \qquad (25)$$

The presence of ferrous ion could even enhance better the degradation of CCl_4 by reaching faster $[Cl^-]_{max,th}$ value as seen in Fig. 4A.
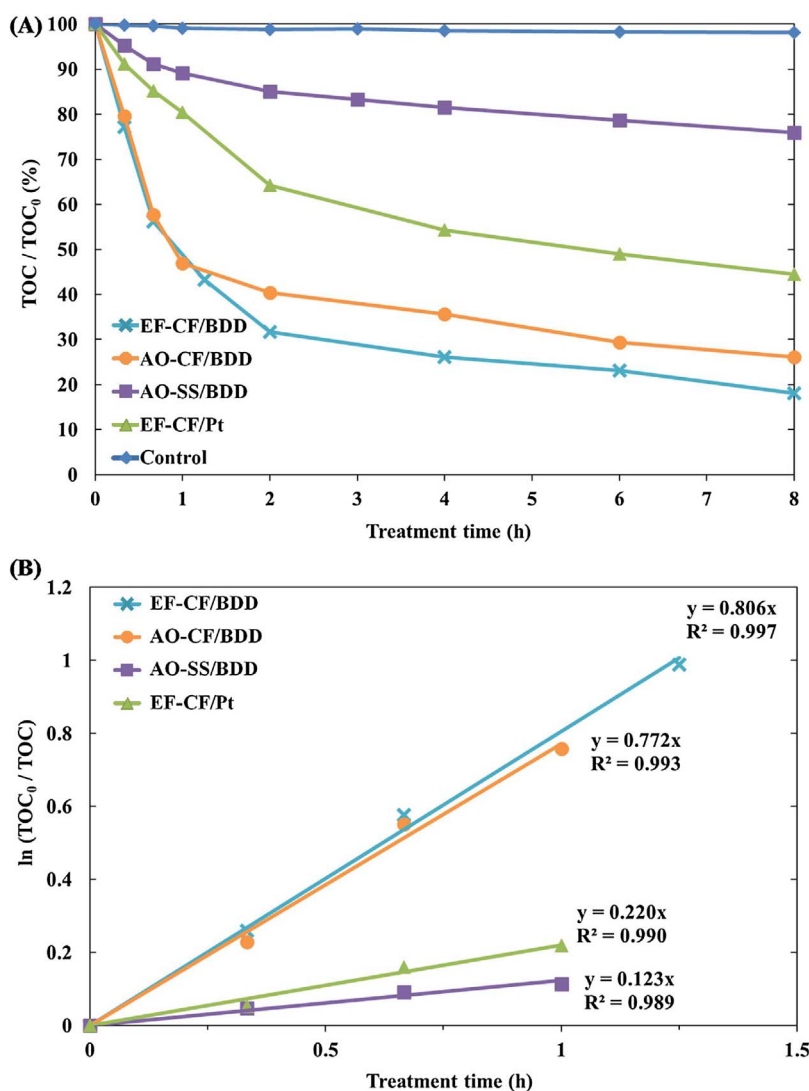
(A)

(B)

Fig. 9. Mineralization of CCl_4 by anodic oxidation and electro-Fenton treatments using different cathodes and anodes. (A), normalized TOC evolution by the initial TOC. (B), determination of the TOC decay rate constants assuming a pseudo-first order kinetic model. EF, electro-Fenton; AO, anodic oxidation; CF, carbon felt; SS, stainless steel; BDD, boron-doped diamond.

This enhancement in CCl_4 degradation rate is due to the formation of homogeneous ·OH formed in bulk solution that react directly with CCl_4, in addition to BDD(·OH) formed at anode surface. In this process, Fenton's reaction (Eq. (25)) is electrocatalyzed by continuous regeneration of Fe^{2+} (catalyst) from electro-reduction of Fe^{3+} ions (Eq. (26)) formed by Fenton's reaction [48]:

$$Fe^{3+} + e^- \rightarrow Fe^{2+} \qquad (26)$$

The difference of efficiency between AO-CF/BDD and EF-CF/BDD experiments was therefore mainly attributed to the action of supplementary ·OH generated in the bulk solution by Fenton reaction (Eq. (25)).

Furthermore, when Pt was used as anode instead of BDD in EF process (EF-CF/Pt cell), the dechlorination rate and yield were higher compared with AO-SS/BDD cell (Fig. 4A). It was also noticed that a plateau of Cl^- concentration was observed in EF-CF/Pt cell experiment, highlighting the accumulation of Cl^- in the solution. In order to better understand this evolution, the chromatograms of anions evolution during EF treatment with Pt anode at different treatment time (0 min, 5 min, 10 min, 20 min, 40 min, 60 min, 120 min, 180 min, 240 min) have been recorded and are represented in Fig. 8. Fig. 8A displays Cl^- peaks at retention time around 1.3 min and major peaks of SO_4^{2-} from the supporting electrolyte (Na_2SO_4) at retention time of 3.1 min, as observed with BDD anode electrolysis. To have a better view of the Cl^- chromatograms, an enlarged picture allows observing the evolution of

Cl^- peaks area and height in Fig. 8B. From 0 min to 40 min of EF treatment, it is clearly seen an increase of peak area, meaning that CCl_4 is progressively degraded into Cl^-. After 40 min of treatment the peaks area barely change, because at this time, the concentration of Cl^- has reached its theoretical level value (0.8 mM). Moreover, no other peak could be observed on the chromatogram whatever the time of treatment, meaning that chloride ions could not be further oxidized into Cl_2, chlorate, perchlorate species on the contrary to BDD experiments. It is also interesting to note that the peaks area of SO_4^{2-} remain the same (50 ± 0.1 mM) whatever the treatment time (Fig. 8C), which underlines that the electrolyte stayed unreactive during the treatment, unlike with BDD treatments. This is in accordance with the low oxidation power of Pt that has a low O_2 evolution overvoltage (1.6 V/SHE) [60]. In this case, ·OH at Pt surface (Pt(·OH)) is chemisorbed and O_2 evolution is the main reaction (Eq. (27a)-(27b)) [47]:

$$Pt + H_2O \rightarrow Pt(·OH) + H^+ + e^- \qquad (27a)$$

$$Pt(·OH) + H_2O \rightarrow Pt + O_2 + 3H^+ + 3e^- \qquad (27b)$$
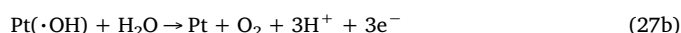
In addition, $[Cl^-]_{max,th}$ (0.8 mM) was reached only after 120 min against around 20 min with AO-CF/BDD and EF-CF/BDD cells. The superiority of AO-CF/BDD cell over EF-CF/Pt cell was attributed to the higher oxidation power of BDD and to the second source of ·OH from peroxone reaction as discussed in Section 3.2.2.

Thus, the only source of ·OH was coming from the electro-Fenton

(A)

(B)

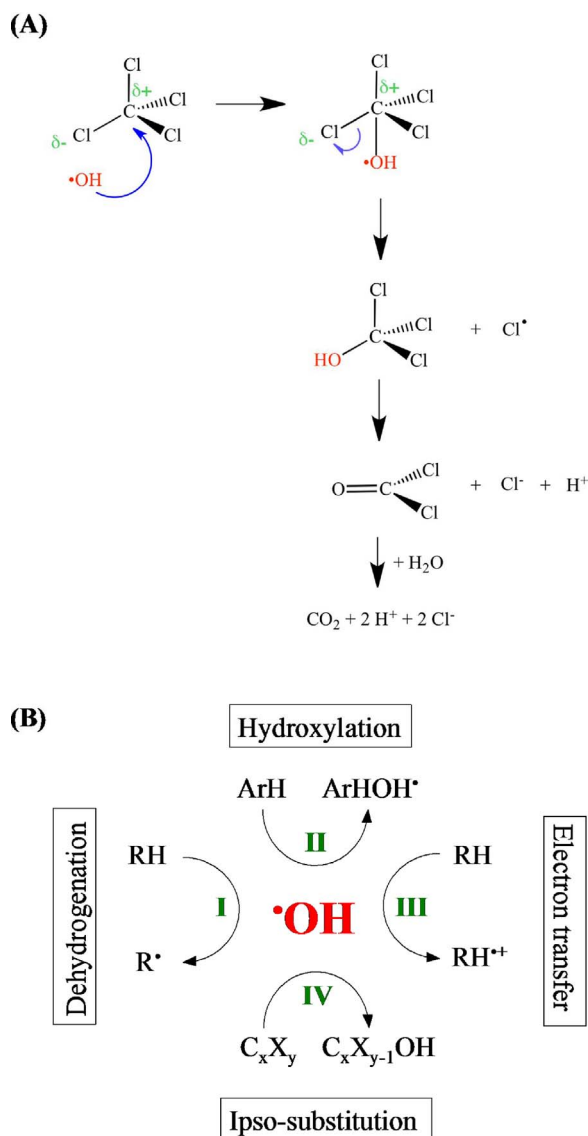**Fig. 10.** Pathways of organic compounds oxidation by $\cdot$OH. (A), CCl_4 oxidation by ipso-substitution with $\cdot$OH. (B), schematic description of the four attack modes of $\cdot$OH with organic compounds. RH, alkane; ArH, aromatic; C_xX_y, perhalogenocarbon compounds.

process through Fenton's reaction in EF-CF/Pt cell. It further emphasized the primary role of homogeneous $\cdot$OH formed by Fenton's reaction as compared to heterogeneous $\cdot$OH formed at BDD surface in AO-SS/BDD cell, because in such diluted solution the electrolysis is controlled by mass transfer rate.

3.2.4. Quantitative comparison between oxidation mechanisms with kinetic rate constants

In order to compare quantitatively each applied condition, a kinetic model has been established (Section 2.3.5). The kinetic rate constants of CCl_4 degradation (k_{app}) have been determined considering a pseudo-first order kinetics for the reaction between CCl_4 and $\cdot$OH by assuming a quasi-stationary state for $\cdot$OH concentration.

Based on Eq. (14), a linear regression allowed determining k_{app} values from the slope of the straight lines (Fig. 4B) that were ranked as follow: AO-SS/BDD ($0.004 \pm 0.001\,min^{-1}$) < EF-CF/Pt ($0.072 \pm 0.003\,min^{-1}$) < AO$-$CF/BDD ($0.171 \pm 0.002\,min^{-1}$) < EF-CF/BDD ($0.298 \pm 0.001\,min^{-1}$). All correlation coefficient (R^2) were higher than 0.989, highlighting the good fitting between experimental data and the pseudo-first order kinetic model. This rank was corroborating the dechlorination

results. It highlights again the primary role of BDD($\cdot$OH)/$\cdot$OH while EF-CF/BDD depicted more than 4 times quicker degradation kinetics due to the three sources of hydroxyl radicals generation (e.g. Fenton, peroxone and anodic oxidation mechanisms co-contributions).
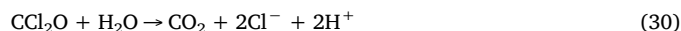
3.3. Mineralization of CCl_4 by EAOPs

The mineralization of CCl_4 was evaluated by monitoring the TOC in the same experimental conditions, e.g. AO-SS/BDD, AO-CF/BDD, EF-CF/BDD and EF-CF/Pt cells (Fig. 9). After 8 h of electrolysis, the following mineralization rank was obtained: AO-SS/BDD ($24 \pm 1.2\%$) < EF-CF/Pt ($55 \pm 1.8\%$) < AO-CF/BDD ($74 \pm 0.9\%$) < EF-CF/BDD ($82 \pm 1.4\%$) (Fig. 9A). In addition, by assuming a pseudo-first order kinetic model for TOC decay [61], the same rank was noticed: AO-SS/BDD ($0.123 \pm 0.011\,h^{-1}$) < EF-CF/Pt ($0.220 \pm 0.013\,h^{-1}$) < AO-CF/BDD ($0.772 \pm 0.012\,h^{-1}$) < EF-CF/BDD ($0.806 \pm 0.010\,h^{-1}$) (Fig. 9B). All correlation coefficient (R^2) values were higher than 0.989, highlighting again the good fitting between experimental data and the pseudo-first order kinetic model.

Knowing that the control experiment has shown negligible TOC removal (2% in 8 h-electrolysis), we could first conclude that CCl_4 was successfully mineralized even with AO-SS/BDD giving the lower production of $\cdot$OH as mentioned previously. Moreover, these ranks of mineralization efficiency were corroborating the degradation kinetics results, demonstrating again the superiority of EF-CF/BDD.

3.4. Proposed reaction pathway

Based on the above finding a reaction pathway for $\cdot$OH action on CCl_4 is proposed (Fig. 10A). For the sake of simplicity, hydroxyl radicals were presented by $\cdot$OH without making explicit the O$-$H bond. First, the presence of Cl atom favors the formation of a dipole between C($\delta+$) and Cl($\delta-$), atoms due to the higher electronegativity of Cl (3.16) compared to C (2.55) according to Pauling scale. Being a strong electrophilic species, $\cdot$OH reacts by ipso-substitution on the C atom (Eq. (28a)) leading to the subsequent formation of trichloromethanol (CCl_3OH) (Eq. (28b)). Trichloromethanol is then decomposed in water into phosgene (CCl_2O) (Eq. (29)) [62]. Finally CCl_2O is quickly hydrolyzed in water by forming CO_2, Cl^- and H^+ (Eq. (30)) [63].

$$CCl_4 + \cdot OH \rightarrow CCl_4(\cdot OH) \tag{28a}$$

$$CCl_4(\cdot OH) \rightarrow CCl_3OH + Cl\cdot \tag{28b}$$

$$CCl_3OH \rightarrow CCl_2O + H^+ + Cl^- \tag{29}$$

$$CCl_2O + H_2O \rightarrow CO_2 + 2Cl^- + 2H^+ \tag{30}$$

Taking into account these considerations, a reaction pathway was therefore proposed for complete degradation of CCl_4 until mineralization, leading to a new attack mode of $\cdot$OH (Fig. 10B). Over the existing attack $\cdot$OH modes, e.g. dehydrogenation, hydroxylation and electron transfer [6,64], a fourth mode, namely "**ipso-substitution**" is proposed. It generally consists of the oxidation of perhalogenocarbon compounds (C_xX_y) into trihalo-alcohol ($C_xX_{y-1}OH$) in a first step. Furthermore, it has been observed a slight continuous decrease of pH during the EAOPs treatments from an initial pH of 3.0 to a final pH of around 2.4 ± 0.2 after 8 h electrolysis with a standard deviation of 0.2 which is due to the kind of applied treatment. This is an evidence of the accumulation of protons formed through the mechanism proposed.

4. Conclusions

In summary, the treatment of CCl_4 in aqueous solution with EAOPs has been investigated for the first time. Upon successful degradation and mineralization of CCl_4 with the unique presence of $\cdot$OH produced by anodic oxidation a new attack mode of $\cdot$OH was proposed on perhalogenocarbon compounds by ipso-substitution of halogen atom with

·OH. The decrease of pH during the electrolysis corroborated the proposed mechanism. The use of electro-Fenton process enhanced significantly the removal efficiency due to generation of supplementary ·OH in the bulk solution.

This fourth oxidation pathway of ·OH should be considered in other areas of research such as in atmospheric studies as some of these perhalogenocarbons are known to be volatile and can be subjected to ·OH reactions.

Furthermore, this new finding opens up many opportunities in environmental protection by offering possibilities of degrading and mineralizing such recalcitrant perhalogenocarbons compounds that are used as solvents, refrigerant, aerosol propellant and representing an environmental issue, such as carbon tetrafluoride, hexafluoroethane, carbon tetrachloride, hexachloroethane, perfluorohexane, and so on, but also cyclic perfluoroalkanes like perfluorooctane, perfluoro-1,3-dimethylcyclohexane and perfluorodecalin. More recently fluorosurfactants such as perfluorooctanesulfonic acid, perfluorononanoic acid and perfluorooctanoic acid have been found into the environment and especially into water bodies. They are employed by some textile companies in emulsion polymerization process to produce fluoropolymers but they have caught recently the attention of regulatory agencies has they are persistent in the environment, toxic and bioaccumulate in the food chain.

In short, this study highlights that perhalogenocarbons compounds should be considered to be eliminated by ·OH generated in EAOPs.

References

[1] S. Gligorovski, R. Strekowski, S. Barbati, D. Vione, Environmental implications of hydroxyl radicals (·OH), Chem. Rev. 115 (2015) 13051–13092.

[2] S. Li, J. Matthews, A. Sinha, Atmospheric hydroxyl radical production from electronically excited NO_2 and H_2O, Science 319 (2008) 1657–1660.

[3] W.H. Rodebush, C.R. Keizer, F.S. McKee, J.V. Quagliano, The reactions of the hydroxyl radical, J. Am. Chem. Soc. 69 (1947) 538–540.

[4] J. Vieceli, L.X. Dang, B.C. Garrett, D.J. Tobias, B. Finlayson-pitts, S. Hunt, P. Jungwirth, Hydroxyl radical at the air – water interface, J. Am. Chem. Soc. 126 (2004) 16308–16309.

[5] P.A. Riley, Free radicals in biology: oxidative stress and the effects of ionizing radiation, Int. J. Radiat. Biol. 65 (1994) 27–33.

[6] L.M. Dorfman, G.E. Adams, Reactivity of the Hydroxyl Radical in Aqueous Solutions, (1973), p. 59.

[7] W.M. Latimer, Oxidation potentials, Soil Sci. 74 (1952) 333.

[8] E.G. Janzen, Y. Kotake, R.D. Hinton, Stabilities of hydroxyl radical spin of PBN-type spin traps, Free Radic. Biol. Med. 12 (1992) 169–173.

[9] W.H. Glaze, J.W. Kang, D.H. Chapin, The chemistry of water-treatment processes involving ozone, hydrogen-peroxide and ultraviolet-radiation, Ozone Sci. Eng. 9 (1987) 335–352.

[10] M.A. Oturan, J.-J. Aaron, Advanced oxidation processes in water/wastewater treatment: principles and applications. A review, Crit. Rev. Environ. Sci. Technol. 44 (2014) 2577–2641.

[11] M. Pelaez, N.T. Nolan, S.C. Pillai, M.K. Seery, P. Falaras, A.G. Kontos, P.S.M. Dunlop, J.W.J. Hamilton, J.A. Byrne, K. O'Shea, M.H. Entezari, D.D. Dionysiou, A review on the visible light active titanium dioxide photocatalysts for environmental applications, Appl. Catal. B Environ. 125 (2012) 331–349.

[12] G.V. Buxton, C.L. Greenstock, W.P. Helman, A.B. Ross, Critical review of rate constants for reactions of hydrated electrons, hydrogen atoms and hydroxyl radicals (·OH/·O$^-$) in aqueous solution, J. Phys. Chem. Ref. Data 17 (1988) 513–886.

[13] Y. Cho, H. Kyung, W. Choi, Visible light activity of TiO_2 for the photoreduction of CCl4 and Cr(VI) in the presence of nonionic surfactant (Brij), Appl. Catal. B Environ. 52 (2004) 23–32.

[14] Y. Cho, H. Park, W. Choi, Novel complexation between ferric ions and nonionic surfactants (Brij) and its visible light activity for CCl_4 degradation in aqueous micellar solutions, J. Photochem. Photobiol. A Chem. 165 (2004) 43–50.

[15] M.C. Gonzalez, G.C. Le Roux, J.A. Rosso, A.M. Braun, Mineralization of CCl_4 by the UVC-photolysis of hydrogen peroxide in the presence of methanol, Chemosphere 69 (2007) 1238–1244.

[16] M. Lee, J. Oh, Sonolysis of trichloroethylene and carbon tetrachloride in aqueous solution, Ultrason. Sonochem. 17 (2010) 207–212.

[17] M. Lim, Y. Son, J. Khim, Frequency effects on the sonochemical degradation of chlorinated compounds, Ultrason. Sonochem. 18 (2011) 460–465.

[18] H. Che, W. Lee, Selective redox degradation of chlorinated aliphatic compounds by Fenton reaction in pyrite suspension, Chemosphere 82 (2011) 1103–1108.

[19] A.L. Teel, R.J. Watts, Degradation of carbon tetrachloride by modified Fenton's reagent, J. Hazard. Mater. 94 (2002) 179–189.

[20] B.A. Smith, A.L. Teel, R.J. Watts, Mechanism for the destruction of carbon tetrachloride and chloroform DNAPLs by modified Fenton's reagent, J. Contam. Hydrol. 85 (2006) 229–246.

[21] J.L. Roberts, D.T. Sawyer, Facile degradation by superoxide ion of carbon tetrachloride, chloroform, methylene chloride, and p, p'-DDT in aprotic media, J. Am. Chem. Soc. 103 (1981) 712.

[22] J.L. Roberts, T.S. Calderwood, D.T. Sawyer, Oxygenation by superoxide ion of CCl_4, $FCCl_3$, $HCCl_3$, p, p'-DDT, and related trichloromethyl substrates ($RCCl_3$) in aprotic solvents, J. Am. Chem. Soc. 105 (1983) 7691–7696.

[23] E. Brillas, I. Sirés, M.A. Oturan, Electro-Fenton process and related electrochemical technologies based on fenton's reaction chemistry, Chem. Rev. 109 (2009) 6570–6631.

[24] M.A. Rodrigo, N. Oturan, M.A. Oturan, Electrochemically assisted remediation of pesticides in soils and water: a review, Chem. Rev. 114 (2014) 8720–8745.

[25] C.A. Martinez-Huitle, M.A. Rodrigo, I. Sires, O. Scialdone, Single and coupled electrochemical processes and reactors for the abatement of organic water pollutants: a critical review, Chem. Rev. 115 (2015) 13362–13407.

[26] I. Sirés, E. Brillas, M.A. Oturan, M.A. Rodrigo, M. Panizza, Electrochemical advanced oxidation processes: today and tomorrow. A review, Environ. Sci. Pollut. Res. Int. 21 (2014) 8336–8367.

[27] F.C. Moreira, R.A.R. Boaventura, E. Brillas, V.J.P. Vilar, Electrochemical advanced oxidation processes: a review on their application to synthetic and real wastewaters, Appl. Catal. B Environ. 202 (2017) 217–261.

[28] E. Mousset, L. Frunzo, G. Esposito, E.D. van Hullebusch, N. Oturan, M.A. Oturan, A complete phenol oxidation pathway obtained during electro-Fenton treatment and validated by a kinetic model study, Appl. Catal. B Environ. 180 (2016) 189–198.

[29] F.C. Moreira, R.A.R. Boaventura, E. Brillas, V.J.P. Vilar, Degradation of trimethoprim antibiotic by UVA photoelectro-Fenton process mediated by Fe (III)?carboxylate complexes, Appl. Catal. B Environ. 162 (2015) 34–44.

[30] F. Yu, M. Zhou, X. Yu, Cost-effective electro-Fenton using modified graphite felt that dramatically enhanced on H_2O_2 electro-generation without external aeration, Electrochim. Acta. 163 (2015) 182–189.

[31] E. Mousset, D. Huguenot, E.D. Van Hullebusch, N. Oturan, G. Guibaud, G. Esposito, M.A. Oturan, Impact of electrochemical treatment of soil washing solution on PAH degradation efficiency and soil respirometry, Environ. Pollut. 211 (2016) 354–362.

[32] D.M. De Araújo, C. Sáez, C.A. Martínez-Huitle, P. Cañizares, M.A. Rodrigo, Influence of mediated processes on the removal of rhodamine with conductive-diamond electrochemical oxidation, Appl. Catal. B Environ. 166–167 (166) (2015) 454—.

[33] F.C. Moreira, R.A.R. Boaventura, E. Brillas, V.J.P. Vilar, Degradation of trimethoprim antibiotic by UVA photoelectro-Fenton process mediated by Fe (III)–carboxylate complexes, Appl. Catal. B Environ. 162 (2015) 34–44.

[34] E. Mousset, N. Oturan, E.D. van Hullebusch, G. Guibaud, G. Esposito, M.A. Oturan, Influence of solubilizing agents (cyclodextrin or surfactant) on phenanthrene degradation by electro-Fenton process – study of soil washing recycling possibilities and environmental impact, Water Res. 48 (2014) 306–316.

[35] N. Oturan, E. Brillas, M.A. Oturan, Unprecedented total mineralization of atrazine and cyanuric acid by anodic oxidation and electro-Fenton with a boron-doped diamond anode, Environ. Chem. Lett. 10 (2012) 165–170.

[36] E. Mousset, N. Oturan, E.D. van Hullebusch, G. Guibaud, G. Esposito, M.A. Oturan, Treatment of synthetic soil washing solutions containing phenanthrene and cyclodextrin by electro-oxidation Influence of anode materials on toxicity removal and biodegradability enhancement, Appl. Catal. B Environ. 160–161 (160) (2014) 666–675.

[37] E. Mousset, Z. Wang, J. Hammaker, O. Lefebvre, Physico-chemical properties of pristine graphene and its performance as electrode material for electro-Fenton treatment of wastewater, Electrochim. Acta 214 (2016) 217–230.

[38] E. Mousset, Z.T. Ko, M. Syafiq, Z. Wang, O. Lefebvre, Electrocatalytic activity enhancement of a graphene ink-coated carbon cloth cathode for oxidative treatment, Electrochim. Acta 222 (2016) 1628–1641.

[39] P.V. Nidheesh, R. Gandhimathi, Trends in electro-Fenton process for water and wastewater treatment: an overview, Desalination 299 (2012) 1–15.

[40] T.X.H. Le, M. Bechelany, S. Lacour, N. Oturan, M.a. Oturan, M. Cretin, High removal efficiency of dye pollutants by electron-Fenton process using a graphene based cathode, Carbon N. Y. 94 (2015) 1003–1011.

[41] E. Mousset, N. Oturan, E.D. van Hullebusch, G. Guibaud, G. Esposito, M.A. Oturan, A new micelle-based method to quantify the Tween 80* surfactant for soil remediation, Agron. Sustain. Dev. 33 (2013) 839–846.

[42] E. Mousset, Z. Wang, O. Lefebvre, Electro-Fenton for control and removal of micropollutants – process optimization and energy efficiency, Water Sci. Technol. 74 (2016) 2068–2074.

[43] F. Sopaj, Study of the Influence of Electrode Material in the Application of Electrochemical Advanced Oxidation Processes to Removal of Pharmaceutical Pollutants from Water, PhD Thesis, University of Paris-Est, 2013.

[44] N. Oturan, J. Wu, H. Zhang, V.K. Sharma, M.A. Oturan, Electrocatalytic destruction of the antibiotic tetracycline in aqueous medium by electrochemical advanced oxidation processes: effect of electrode materials, Appl. Catal. B Environ. 140–141 (140) (2013) 92—.

[45] A.J. Bard, R. Parsons, J. Jordan, Standard Potentials in Aqueous Solutions, (1985).

[46] B. Marselli, J. Garcia-Gomez, P.-A. Michaud, M.A. Rodrigo, C. Comninellis, Electrogeneration of hydroxyl radicals on boron-doped diamond electrodes, J. Electrochem. Soc. 150 (2003) D79–D83.

[47] M. Panizza, G. Cerisola, Direct and mediated anodic oxidation of organic pollutants, Chem. Rev. 109 (2009) 6541–6569.

[48] I. Sirés, J.A. Garrido, R.M. Rodríguez, E. Brillas, N. Oturan, M.A. Oturan, Catalytic behavior of the Fe^{3+}/Fe^{2+} system in the electro-Fenton degradation of the antimicrobial chlorophene, Appl. Catal. B Environ. 72 (2007) 382–394.

[49] M.E.H. Bergmann, J. Rollin, T. Iourtchouk, The occurrence of perchlorate during drinking water electrolysis using BDD anodes, Electrochim. Acta 54 (2009)

2102–2107.

[50] A. Vacca, M. Mascia, S. Palmas, A. Da Pozzo, Electrochemical treatment of water containing chlorides under non-ideal flow conditions with BDD anodes, J. Appl. Electrochem. 41 (2011) 1087–1097.

[51] C. Salazar, I. Sires, R. Salazar, H. Mansilla, C. Zaror, Treatment of cellulose bleaching effluents and their filtration permeates by anodic oxidation with H_2O_2 production, J. Chem. Technol. Biotechnol. 90 (2015) 2017–2026.

[52] E. Lacasa, J. Llanos, P. Cañizares, M.A. Rodrigo, Electrochemical denitrificacion with chlorides using DSA and BDD anodes, Chem. Eng. J. 184 (2012) 66–71.

[53] J. Davis, J.C. Baygents, J. Farrell, Understanding persulfate production at boron doped diamond film anodes, Electrochim. Acta 150 (2014) 68–74.

[54] K. Serrano, P.A. Michaud, C. Comninellis, A. Savall, Electrochemical preparation of peroxodisulfuric acid using boron doped diamond thin film electrodes, Electrochim. Acta 48 (2002) 431–436.

[55] G.P. Anipsitakis, M.A. Gonzalez, Cobalt-mediated activation of peroxymonosulfate and sulfate radical attack on phenolic compounds. implications of chloride ions, Environ. Sci. Technol. 40 (2006) 1000–1007.

[56] G. Merényi, J. Lind, S. Naumov, C. von Sonntag, Reaction of ozone with hydrogen peroxide (peroxone process): a revision of current mechanistic concepts based on thermokinetic and quantum-chemical considerations, Environ. Sci. Technol. 44 (2010) 3505–3507.

[57] C.A. Martínez-Huitle, E. Brillas, Electrochemical alternatives for drinking water disinfection, Angew. Chem. Int. Ed. Engl. 47 (2008) 1998–2005.

[58] Y. Honda, T.A. Ivandini, T. Watanabe, K. Murata, Y. Einaga, An electrolyte-free system for ozone generation using heavily boron-doped diamond electrodes, Diam. Relat. Mater. 40 (2013) 7–11.

[59] P. Christensen, T. Yonar, K. Zakaria, The electrochemical generation of ozone: a review, Ozone Sci. Eng. 35 (2013) 149–167.

[60] A. Kapałka, G. Fóti, C. Comninellis, Kinetic modelling of the electrochemical mineralization of organic pollutants for wastewater treatment, J. Appl. Electrochem. 38 (2008) 7–16.

[61] N. Oturan, E.D. Van Hullebusch, H. Zhang, L. Mazeas, H. Budzinski, K. Le Menach, M.A. Oturan, Occurrence and removal of organic micropollutants in landfill leachates treated by electrochemical advanced oxidation processes, Environ. Sci. Technol. 49 (2015) 12187–12196.

[62] K. Brudnik, D. Wójcik-pastuszka, J.T. Jodkowski, J. Leszczynski, Theoretical study of the kinetics and mechanism of the decomposition of trifluoromethanol trichloromethanol, and tribromomethanol in the gas phase, J. Mol. Model. 14 (2008) 1159–1172.

[63] R. Mertens, C. von Sonntag, J. Lind, G. Merenyi, A kinetic study of the hydrolysis of phosgene in aqueous solution by pulse radiolysis, Angew. Chem. Int. Ed. Engl. 33 (1994) 1259–1261.

[64] C. Von Sonntag, Advanced oxidation processes: mechanistic aspects, Water Sci. Technol. 58 (2008) 1015–1021.